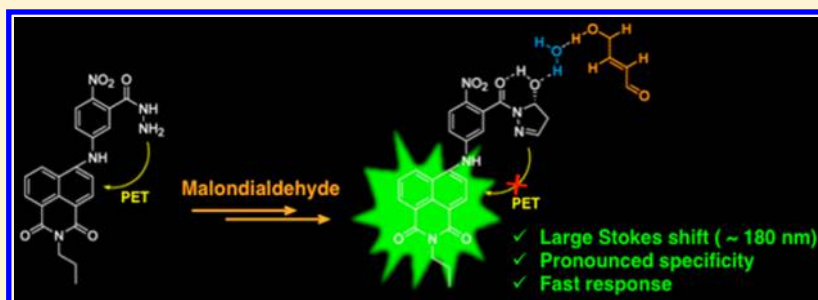


Toward a Biomarker of Oxidative Stress: A Fluorescent Probe for Exogenous and Endogenous Malondialdehyde in Living Cells

Jin Chen,^{†,||} Lingyu Zeng,^{‡,||} Tian Xia,[§] Shuang Li,[†] Tengfei Yan,[†] Song Wu,^{*,†} Guofu Qiu,[†] and Zhihong Liu^{*,‡}

[†]School of Pharmaceutical Sciences, [‡]Key Laboratory of Analytical Chemistry for Biology and Medicine (Ministry of Education), College of Chemistry and Molecular Sciences, and [§]College of Life Science, Wuhan University, Wuhan, Hubei 430072, China

S Supporting Information



ABSTRACT: Malondialdehyde (MDA) is a significant biomarker of oxidative stress. Variations of MDA level in biological systems often represent pathological changes that are related with many types of diseases. Although a variety of techniques have been developed for MDA detection, the probing of this biomarker in living cells remains unexplored. Herein, we report a turn-on fluorescent probe, **MDAP-1**, with a synergistic photoinduced electron transfer (PET)-hydrogen bonding mechanism, which for the first time realizes MDA sensing under physiological conditions with excellent sensitivity and specificity. The probe responds to MDA with a fluorescence enhancement factor (FEF) of up to >170-fold and a large Stokes shift (~180 nm). Further biological evaluations show that **MDAP-1** is able to detect both endogenous and exogenous MDA in living cells. It can be used to track the generation of MDA under oxidative stress, as stimulated by H₂O₂. We believe the results of this work will be helpful to the studies of MDA-related biological events and the elucidation of the underlying pathological mechanism in the future.

Oxidative stress, defined as a disturbance in the balance between the production of reactive oxygen species (ROS) and antioxidant defenses in a biological system, has long been an active research field as it is believed to be a major pathophysiological mechanism in mediating many disease states.¹ A byproduct of polyunsaturated fatty acid peroxidation caused by ROS, malondialdehyde (MDA) is regarded as a typical biomarker of oxidative stress. Since it has high reactivity, MDA is toxic, potentially mutagenic, and atherogenic due to its reactions with biomolecules such as proteins² and nucleic acids.^{3–5} Alteration of MDA level in the living organism often reflects pathological changes,^{6–8} which have been verified in various types of illnesses such as leukemia,⁹ diabetes,¹⁰ cancer,¹¹ cardiovascular disease,¹² age-related macular degeneration,¹³ asthma,¹⁴ atherosclerosis,¹⁵ and liver disease.¹⁶ Therefore, it is of great significance to detect MDA to monitor the progression of the diseases and elucidate the underlying pathology mechanisms in living subjects.

Currently, the detection methods for MDA include the most widely used 2-thiobarbituric acid (TBA) assay^{17,18} and newly developed techniques such as liquid chromatography,^{19–24} electrophoresis,^{25–27} gas chromatography,^{28,29} and Raman spectroscopy.³⁰ However, almost all these methods suffer from rather tedious chemical derivatizations usually under harsh

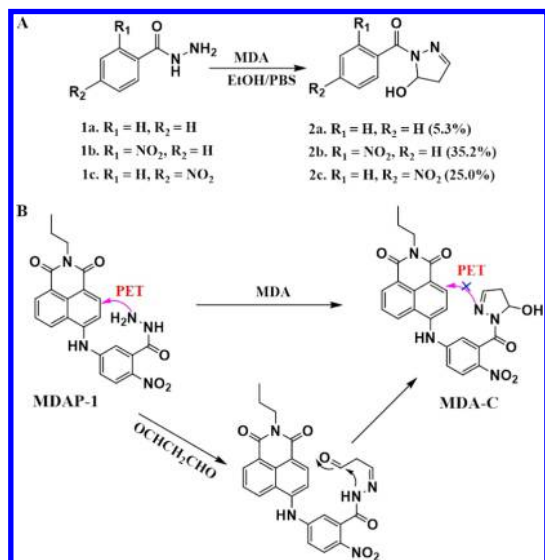
conditions like strong acidity and/or elevated temperature; thus, they are applicable only in body fluid samples like serum and urine. Meanwhile, MDA-related *in vivo* studies, currently, are based on bulky and expensive MDA-specific antibody that predominantly works on the cell membrane.¹³ Clearly, there is a great demand for the development of cheap, cell permeable, and highly selective small molecule fluorescent probes that enable direct visualization and minimally interfere with the corresponding biological processes. Herein, we report the first fluorescent probe for MDA working under physiological conditions and suitable for probing both exogenous and endogenous MDA in living cells.

Aiming to develop a fluorescent probe for intracellular MDA imaging, we initially studied the model reaction of MDA with benzohydrazide (compound **1a**, Scheme 1) in aqueous solution at room temperature. It is known that hydrazide is reliably condensed with aldehyde under acidic conditions, but the reaction between benzohydrazide and two carbonyl compound MDA under physiological conditions still needs to be elucidated. We also envisioned that the structural modification

Received: May 31, 2015

Accepted: July 22, 2015

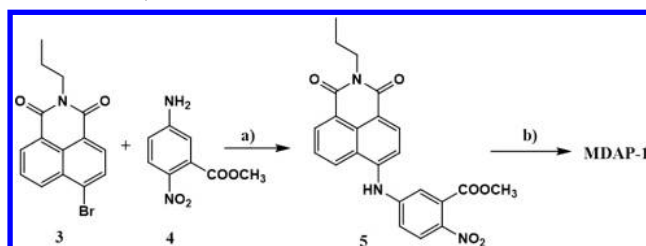
Scheme 1. (A) Model Reactions of Benzohydrazide Derivatives and MDA; (B) The Design Principle and the Reaction Mechanism of MDA Probe (MDAP-1)



of benzohydrazide might be able to influence the reaction process. It is reported that 2,4-dinitrophenylhydrazine (DNPH), a MDA derivatization agent, shows excellent reactivity toward MDA possibly attributed to the very strong electron-withdrawing effect of the two nitro groups.³¹ We hypothesized that this effect may also influence the reaction between benzohydrazide and MDA. To this end, we designed and synthesized two hydrazide analogues bearing an electron-withdrawing nitro group at the *ortho* and *para* position (compound **1b** and **1c**, Scheme 1A), respectively. MDA was freshly prepared from acid hydrolysis of 1,1,3,3-tetrahydroxypropane (TEP) according to the literature.²³ The reactions between MDA and equivalent benzohydrazide derivatives were carried out in ethanol-PBS (1/1, v/v, 50 mM, pH 7.4) component solvent with 30 min of stirring at room temperature. After isolation, a series of 4,5-dihydro-1H-pyrazole derivatives (**2a–2c**) with similar structures was obtained at the yields of 5.3% for compound **2a**, 35.2% for **2b**, and 25.0% for **2c**, respectively (for the details please, see the Supporting Information). The cyclization processes during the reactions are confirmed by the chemical shifts of ca. 2.8 and 3.1 ppm (**2a–2c**) assigned to the two protons of methylene on the 4,5-dihydro-1H-pyrazole rings (for the ¹H NMR data, please see the Supporting Information). From the perspective of the reaction mechanism, this type of reaction may involve first condensation of the terminal amine group on the hydrazide with an aldehyde group of MDA, followed by an additional reaction between the other aldehyde group of MDA and the imino group to give the cyclized hemiaminal product, without further dehydration that often occurs under acidic conditions. Apparently, the electron-withdrawing effect and the substitution position of the nitro group profoundly affect the reaction kinetics as we speculated. We then used the most reactive *ortho*-nitro substituted benzohydrazide as the recognition moiety to construct the probe (MDAP-1) by linking the fluorophore of 1,8-naphthalimide via an imino group. Since the existence of lone-pair electrons on hydrazine of MDAP-1, this probe should have weak fluorescence (photoinduced electron transfer (PET) mechanism). However, after the reaction with MDA, the

expected cyclized product MDA-C may turn on the fluorescence because of the interruption of the PET process (the reaction mechanism between MDAP-1 and MDA and the fluorescence turn-on mechanism upon the reaction are shown in Scheme 1B). Using compound **3** as the starting material, we readily synthesized the ester intermediates **5** via Buchwald-Hartwig amination³² by reacting with the amine **4** in the presence of palladium catalyst under basic conditions. The following treatment by refluxing **5** with a large excess amount of hydrazine offered the desired compound MDAP-1 (Scheme 2). All compounds were fully characterized by ¹H NMR, ¹³C NMR, HRMS, and HPLC (for the details, please see the Supporting Information).

Scheme 2. Synthetic Route of the Probe^a



^aReagents and conditions: (a) Pd₂(dba)₃, Cs₂CO₃, toluene, BINAP, reflux overnight; (b) N₂H₄·H₂O, CH₃OH, reflux overnight.

Next, we studied the optical properties and fluorescence response to MDA of the probe MDAP-1. In DMSO-PBS component solvent (1/9, v/v, 50 mM, pH 7.4), MDAP-1 (10 μM) showed extremely weak intrinsic fluorescence, suggesting that the luminescence of 1,8-naphthalimide is efficiently quenched by the recognition moiety. Interestingly, upon reaction with MDA, MDAP-1 exhibited unexpected fluorescence enhancement at two separate excitation/emission peaks of 370/553 and 480/520 nm, respectively. Fluorescence titration of MDAP-1 with different concentrations of MDA, as shown in Figure 1a,b, exhibited the maximum fluorescence enhancement factor (FEF) at 553 and 520 nm, reaching up to 174-fold and 52-fold in the presence of 1 mM MDA, respectively (Figure 1c). In addition, both the FEFs are linearly dependent on the concentration of MDA within the range of 2–200 μM (Figure 1d), with a detection limit of ca. 0.6 μM (S/N = 3, *n* = 11), indicating the potential use of MDAP-1 for quantitative detection of MDA under physiological conditions. The above observations also provide a useful tool for alternative two-channel detection of MDA with this probe. Particularly, the exceptional Stokes shift of the 553 nm emission (~180 nm) in an aqueous environment ensures a thorough elimination of spectral cross talk, which is significant for bioimaging, and it was thus chosen for the subsequent fluorescence and cell imaging studies.

In order to elucidate the mechanism of this unique two-channel fluorescence response, we settled another reaction by mixing and stirring MDAP-1 with an equivalent amount of MDA for 1 h at room temperature. Acetonitrile-PBS component solvent (1/1, v/v, 50 mM, pH 7.4) was used in this reaction to ensure the solubility of MDAP-1. The fluorescent product was isolated and found to be MDA-C as expected (see the Supporting Information). We found that MDA-C showed a single emission band with the maximum excitation/emission located at 480/520 nm in DMSO-PBS solution (1/9, v/v, 50 mM, pH 7.4). Surprisingly, when we

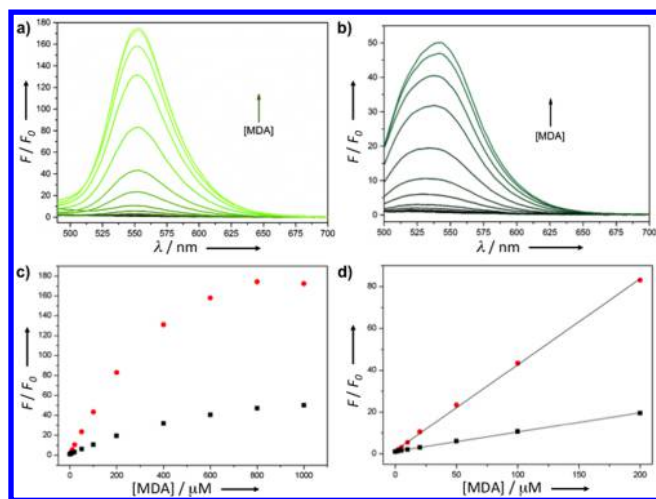


Figure 1. Fluorescence spectra of MDAP-1 (10 μM) in the presence of an increasing amount of MDA (0, 2, 5, 10, 20, 50, 100, 200, 400, 600, 800, and 1000 μM) with (a) 370 nm and (b) 480 nm excitation. (c) The corresponding titration curves acquired at 553 nm (red dots) and 520 nm (black squares) separately. (d) The partial data of (c) with linear responses at low MDA concentrations. All the experiments were performed in DMSO-PBS component solvent (1/9, v/v, 50 mM, pH 7.4). F and F_0 represent the emission intensity of MDAP-1 in the presence and absence of MDA, respectively.

added excessive MDA to the solution, the 520 nm emission peak immediately shifted to 553 nm along with appearance of a new maximum excitation wavelength of 370 nm (Figure S1a). Clearly, there was a fast interaction between MDA-C and MDA. We speculate that it is less likely to be covalent bonding since it is such a quick process. To interpret this interaction, we prepared solid MDA and performed nuclear Overhauser effect spectroscopy (NOESY) analysis on the product, which suggested that the weak interaction could be hydrogen bonding between MDA-C and MDA in the presence of H_2O molecule (NOESY spectra, related analysis, and proposed structures are shown in Figures S2–S6). A control experiment by mixing solid MDA and MDA-C in nonaqueous solvent, chloroform, showed no significant fluorescence variation, confirming the role of H_2O in hydrogen bonding and the impact on the fluorescence emission as well (Figure S1b). According to the above results, a synergistic mechanism of the fluorescence response was proposed and depicted in Scheme 3. The turn-on of 480/520 nm may due to the PET mechanism as discussed before, and the rapid formation of the ternary complex of MDA-C, MDA, and H_2O via hydrogen bonding causes the red shift of the

Scheme 3. Proposed Synergistic Turn-on Mechanism for MDAP-1



emission to 553 nm with largely enhanced fluorescence intensity.

The effect of pH on the fluorescence of MDAP-1 as well as the MDA-MDAP-1 reaction was then examined. The results show that the fluorescence of the species is insensitive to pH in the physiological range of 6.5–7.5 (Figure S7). The time-dependence studies show that fluorescence enhanced quickly (ca. 60-fold at 5 min and 110-fold at 10 min), and it reaches the plateau in only 30 min (Figure S8). Considering the high reactivity and fast degradation of intracellular MDA,³³ such a quick response can be essentially useful for MDA imaging in living systems.

We subsequently tested the specificity of MDAP-1 toward MDA. Three aspects of potential interfering agents were tested including the ions (M^{2+} : Mg^{2+} , Cd^{2+} , Ca^{2+} , Mn^{2+} , Zn^{2+} , Hg^{2+} , Fe^{2+} , Cu^{2+}), the reactive oxygen species (ROS: H_2O_2 , ClO^- , O_2^- , $\cdot\text{OH}$, $^1\text{O}_2$), and reactive carbonyl species (RCS: acetone, acetaldehyde, glutaraldehyde, acetylacetone, formaldehyde, glyoxal, methylglyoxal), in which the latter two are known to ascend under oxidative stress. As Figure 2 shows, none of these species caused significant fluorescence enhancement of MDAP-1. The above results have suggested the pronounced specificity of the probe.

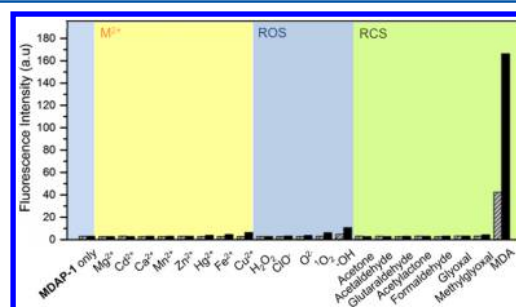


Figure 2. Responses of 10 μM MDAP-1 to M^{2+} , ROS, RCS, and MDA at 0.1 and 1 mM, shown as pattern and black bar, respectively. All the experiments were performed in DMSO-PBS component solvent (1/9, v/v, pH 7.4). Data were acquired at 553 nm with 370 nm excitation.

Before utilizing MDAP-1 in bioimaging, we tested its cytotoxicity by the tetrazolium-based colorimetric assay (MTT assay). The result shows that the survival rate of HeLa cells incubated with 1–10 μM MDAP-1 for 24 h was almost the same with that of the control group containing DMSO only (Figure S9), revealing the limited cytotoxicity of the probe.

As the initial step of bioapplication, we first incubated HeLa cells with 5 μM MDAP-1 for 30 min. Compared to the negative control group without loading the probe (Figure S10), the probe-loaded cells exhibited faint fluorescence in the cytosol (Figure 3a), which might be resulting from the intrinsic intracellular MDA. To figure this out, we set another two control groups pretreated with the MDA scavenger, L-carnosine,³⁴ for 1 h (Figure 3b,c, with 0.2 and 2 mM L-carnosine, respectively). Compared to Figure 3a, the fluorescence of L-carnosine-treated cells was slightly weakened. These observations demonstrate that MDAP-1 is able to recognize the low-concentration basal MDA in cells. Further experiments were designed to check the ability of MDAP-1 to recognize exogenous MDA, in which three groups of probe-loaded cells were further incubated with different amounts (0.1, 0.2, and 0.5 mM) of external MDA for 30 min (Figure 3d–f). It

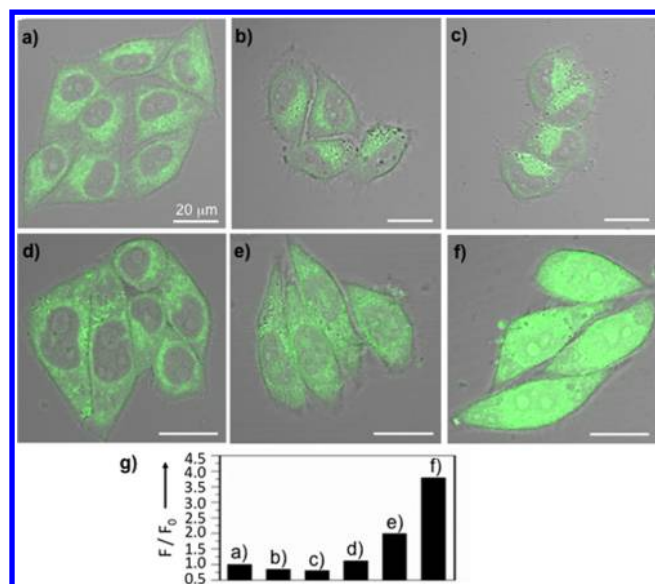


Figure 3. Merged images of HeLa cells (a) incubated at 37 °C for 30 min with 5 μ M MDAP-1 and (b) pretreated with 0.2 mM or (c) 2 mM L-carnosine for 1 h. Probe-loaded cells further incubated with (d) 0.1 mM, (e) 0.2 mM, and (f) 0.5 mM external MDA for 30 min. Images were collected at 500–650 nm upon excitation at 400 nm. Scale bar: 20 μ m. Cells shown are representative images from replicate experiments ($n = 5$). (g) Normalized fluorescence intensity of images (a–f), in which F_0 and F means the fluorescence intensity without and with pre/post-treatments, respectively. The images from bright-field and fluorescent channels are shown in Figures S11–S12.

is clearly seen that the fluorescence intensities of the cells were elevated along with an increase of MDA concentration.

Ultimately, we tried using MDAP-1 to track the endogenously generated MDA under oxidative stress, with H_2O_2 as a stimulant.³⁵ Three groups of HeLa cells were first loaded with 5 μ M MDAP-1. In the first group, 0.5 mM (final concentration) H_2O_2 solution was added into the confocal dish (the cells before and after stimulation are presented in Figure 4a,b). As tracked in circles A and B, the fluorescence signals of both circles increased shortly after H_2O_2 addition. The quantitative intensities are integrated and drawn in Figure 4g (curves A and B). A similar trend was also observed at a lower H_2O_2 concentration of 0.1 mM for the second group, as shown in Figure 4c,d and curves C and D in Figure 4g, but with a much less degree of fluorescence enhancement. The fluorescence variation represented in these two groups vividly demonstrated that MDAP-1 was able to probe endogenously generated MDA upon H_2O_2 stimulation. To further confirm this conclusion, we designed the third group by suppressing the oxidative stress to indirectly block the generation of MDA. In this experiment, a natural antioxidant, ascorbic acid, was mixed with an equal amount of H_2O_2 and added into the medium. As expected, no significant fluorescence enhancement was observed during the time course, as shown by Figure 4e,f and curves E and F in Figure 4g. This observation also provides a direct proof for the therapeutic effect of ascorbic acid against oxidative stress.

In summary, we have proposed a turn-on fluorescent probe (MDAP-1) for MDA with a > 170-fold FEF and an exceptional Stokes shift based on a synergistic PET-hydrogen bonding mechanism. The probe possesses excellent specificity over a variety of metal ions, ROS, and RCS. MDAP-1 enables

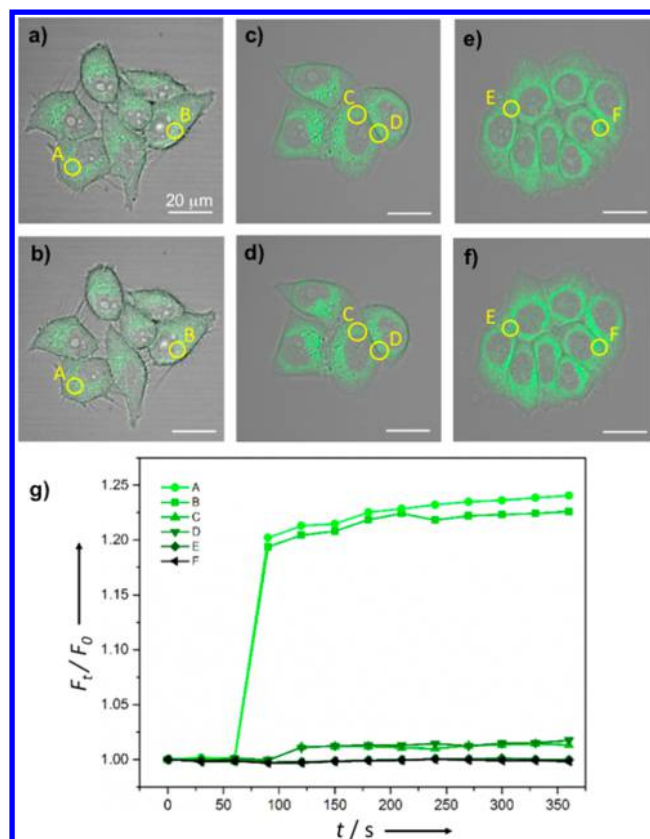


Figure 4. Merged images of HeLa cells (a) before and (b) after 0.5 mM H_2O_2 stimulation (added at 1 min); (c) before and (d) after 0.1 mM H_2O_2 stimulation (added at 1.5 min). Probe-loaded cells (e) before and (f) after adding the mixture of 0.5 mM ascorbic acid and 0.5 mM H_2O_2 (added at 1.5 min). (g) Normalized fluorescence intensity from circles A–F as a function of time. Fluorescence (F_t) was collected with 30 s intervals for the duration of 6 min under *xyt* mode, and F_0 was the fluorescence intensity at $t = 0$. Images were collected at 500–650 nm upon excitation at 400 nm. Scale bar: 20 μ m. Cells shown are representative images from replicate experiments ($n = 5$).

quantitative detection of MDA *in vitro* at low concentration ranges. Meanwhile, MDAP-1 is able to recognize both exogenous and endogenous MDA in living cells. It is also applicable in probing MDA under oxidative stress. To the best of our knowledge, this is the first fluorescent probe for MDA working under physiological conditions, which can be beneficial to the studies of MDA-related biological events.

■ ASSOCIATED CONTENT

Supporting Information

The Supporting Information is available free of charge on the ACS Publications website at DOI: 10.1021/acs.analchem.5b02032.

Synthesis procedures, characterization data, cell imaging, cytotoxicity, and additional figures (PDF)

■ AUTHOR INFORMATION

Corresponding Authors

*E-mail: songwu@whu.edu.cn.

*E-mail: zhhlui@whu.edu.cn.

Author Contributions

[†]J.C. and L.Z. contributed equally.

Notes

The authors declare no competing financial interest.

■ ACKNOWLEDGMENTS

We thank Prof. Shenping Yang and Dr. Yousheng Cai for helpful discussion on NMR analysis. Financial support from the National Natural Science Foundation of China (no. 21375098) is acknowledged.

■ REFERENCES

- (1) Gorrini, C.; Harris, I. S.; Mak, T. W. *Nat. Rev. Drug Discovery* **2013**, *12*, 931–947.
- (2) Hyvarinen, S.; Uchida, R.; Varjosalo, M.; Jokela, R.; Jokiranta, T. *S. J. Biol. Chem.* **2014**, *289*, 4295–4306.
- (3) Chaudhary, A. K.; Nokubo, M.; Reddy, G. R.; Yeola, S. N.; Morrow, J. D.; Blair, I. A.; Marnett, L. J. *Science* **1994**, *265*, 1580–1582.
- (4) Otteneder, M. B.; Knutson, C. G.; Daniels, J. S.; Hashim, M.; Crews, B. C.; Remmel, R. P.; Wang, H.; Rizzo, C.; Marnett, L. J. *Proc. Natl. Acad. Sci. U. S. A.* **2006**, *103*, 6665–6669.
- (5) Riggins, J. N.; Pratt, D. A.; Voehler, M.; Daniels, J. S.; Marnett, L. J. *J. Am. Chem. Soc.* **2004**, *126*, 10571–10581.
- (6) Willis, M. S.; Klassen, L. W.; Carlson, D. L.; Brouse, C. F.; Thiele, G. M. *Int. Immunopharmacol.* **2004**, *4*, 885–899.
- (7) Niedernhofer, L. J.; Daniels, J. S.; Rouzer, C. A.; Greene, R. E.; Marnett, L. J. *J. Biol. Chem.* **2003**, *278*, 31426–31433.
- (8) Cline, S. D.; Riggins, J. N.; Tornaletti, S.; Marnett, L. J.; Hanawalt, P. C. *Proc. Natl. Acad. Sci. U. S. A.* **2004**, *101*, 7275–7280.
- (9) Petrola, M. J.; de Castro, A. J. M.; Pitomberia, M. H.; Barbosa, M. C.; Quixada, A. T.; Duarte, F. B.; Goncalves, R. P. *Rev. Bras. Hematol. Hemoter.* **2012**, *34*, 352–355.
- (10) Jain, S. K.; McVie, R.; Smith, T. *Diabetes Care* **2000**, *23*, 1389–1394.
- (11) Dillioglugil, M. O.; Mekik, H.; Muezzinoglu, B.; Ozkan, T. A.; Demir, C. G.; Dillioglugil, O. *Int. Urol. Nephrol.* **2012**, *44*, 1691–1696.
- (12) Boaz, M.; Matas, Z.; Biro, A.; Katzir, Z.; Green, M.; Fainaru, M.; Smetana, A. *Kidney Int.* **1999**, *56*, 1078–1083.
- (13) Weismann, D.; Hartvigsen, K.; Lauer, N.; Bennett, K. L.; Scholl, H. N.; Issa, P. C.; Cano, M.; Brandstatter, H.; Tsimikas, S.; Skerka, C.; Superti-Furga, G.; Handa, J. T.; Zipfel, P. F.; Witztum, J. L.; Binder, C. J. *Nature* **2011**, *478*, 76–81.
- (14) Romieu, I.; Barraza-Villarreal, A.; Escamilla-Nunez, C.; Almstrand, A. C.; Diaz-Sanchez, S.; Sly, P. D.; Olin, A. C. *J. Allergy Clin. Immunol.* **2008**, *121*, 903–909.
- (15) Tajika, K.; Okamatsu, K.; Takano, M.; Inami, S.; Yamamoto, M.; Murakami, D.; Kobayashi, N.; Ohba, T.; Hata, N.; Seino, Y. *Circ. J.* **2012**, *76*, 2211–2217.
- (16) Smathers, R. L.; Galligan, J. J.; Stewart, B. J.; Petersen, D. R. *Chem.-Biol. Interact.* **2011**, *192*, 107–112.
- (17) Ohkawa, H.; Ohishi, N.; Yagi, K. *Anal. Biochem.* **1979**, *95*, 351–358.
- (18) Janero, D. R. *Free Radical Biol. Med.* **1990**, *9*, 515–540.
- (19) Czauderna, M.; Kowalczyk, J.; Marounek, M. *J. Chromatogr. B: Anal. Technol. Biomed. Life Sci.* **2011**, *879*, 2251–2258.
- (20) Cheng, G. W.; Wu, H. L.; Huang, Y. L. *Talanta* **2009**, *79*, 1071–1075.
- (21) Bergamo, P.; Fedele, E.; Balestrieri, M.; Abrescia, P.; Ferrara, L. *J. Agric. Food Chem.* **1998**, *46*, 2171–2176.
- (22) Rezaei, Z.; Jamshidzadeh, A.; Sanati, E. *Anal. Methods* **2013**, *5*, 2995–2999.
- (23) Tsuruta, Y.; Date, Y.; Tonogaito, H.; Sugihara, N.; Furuno, K.; Kohashi, K. *Analyst* **1994**, *119*, 1047–1050.
- (24) Li, P.; Ding, G.; Deng, Y.; Punyapitak, D.; Li, D.; Cao, Y. *Free Radical Biol. Med.* **2013**, *65*, 224–231.
- (25) Zinellu, A.; Sotgia, S.; Deiana, L.; Carru, C. *Electrophoresis* **2011**, *32*, 1893–1897.
- (26) Zinellu, A.; Sotgia, S.; Deiana, L.; Carru, C. *Anal. Bioanal. Chem.* **2011**, *399*, 2855–2861.
- (27) Cooley, J. C.; Lunte, C. E. *Electrophoresis* **2011**, *32*, 2994–2999.
- (28) Shin, H. S. *J. Chromatogr. B: Anal. Technol. Biomed. Life Sci.* **2009**, *877*, 3707–3711.
- (29) Stalikas, C. D.; Konidari, C. N. *Anal. Biochem.* **2001**, *290*, 108–115.
- (30) Zhang, D. M.; Haputhanthri, R.; Ansar, S. M.; Vangala, K.; De Silva, H. I.; Sygula, A.; Saebo, S.; Pittman, C. U., Jr. *Anal. Bioanal. Chem.* **2010**, *398*, 3193–3201.
- (31) Pilz, J.; Meineke, I.; Gleiter, C. H. *J. Chromatogr., Biomed. Appl.* **2000**, *742*, 315–325.
- (32) Wolfe, J. P.; Wagaw, S.; Buchwald, S. L. *J. Am. Chem. Soc.* **1996**, *118*, 7215–7216.
- (33) Agarwal, R.; Chase, S. D. *J. Chromatogr. B: Anal. Technol. Biomed. Life Sci.* **2002**, *775*, 121–126.
- (34) Hipkiss, A. R.; Preston, J. E.; Himsworth, D. M.; Worthington, V. C.; Abbot, N. J. *Neurosci. Lett.* **1997**, *238*, 135–138.
- (35) Nakamura, J.; Purvis, E. R.; Swenberg, J. A. *Nucleic Acids Res.* **2003**, *31*, 1790–1795.